CREEP DEFORMATION OF INCONEL ALLOY 718

IN THE 650°C TO 760°C TEMPERATURE REGIME

R.W. Hayes

Metals Technology, Inc.
19801 Nordhoff Street
Northridge, California 91324

Abstract

The steady-state creep behavior of a commercial grade Inconel alloy 718 has been studied over the temperature range of 650°C to 760°C at initial applied stress levels ranging from 276 MPa up to 724 MPa. Two age heat treatments were also compared and found to exhibit comparable stress exponents and apparent creep activation energies indicating that the fundamental steady-state creep deformation mechanisms were independent of age heat treatment. In the case of both heat treatments, the creep stress exponents and activation energies are significantly higher than those of pure Ni (i.e. n=5 and Q_c=Q_l=280 kJ/mole) assuming dislocation creep as the rate limiting deformation mechanism. The high stress exponents reflect the strengthening imparted by the γ'' precipitates while the high creep activation energy is suggested to reflect multi-component diffusion controlled γ'' precipitate coarsening as rate limiting for steady-state creep deformation.

Introduction

INCONEL alloy 718 (IN 718) is a precipitation strengthened iron-nickel based superalloy containing about 5.3 wt pct niobium which exhibits good strength, ductility and fatigue resistance up to about 650°C[1]. This alloy is currently used as a disc material in existing air breathing gas turbine jet engines. This alloy is unique in that after commercial solution treat and precipitation heat treatments, two types of precipitate phases co-exist within the Ni rich gamma matrix. These two phases are gamma prime (γ') Ni_3 (Al, Ti, Nb) having the FCC $L1_2$ crystal structure and the gamma double prime (γ'') Ni_3 (Nb, Al, Ti) having the BCT DO_{22} crystal structure[1]. The γ'' phase is considered to be the predominant strengthening phase of IN 718 and it posseses a higher lattice misfit with the gamma phase than does the γ'[2]. This higher lattice misfit exhibited by the BCT γ'' increases the tendency toward precipitate instability and thus coarsening with long term exposures at elevated temperatures. This condition sets the upper bound use temperature of 650°C for this alloy. Collier et al have recently reviewed the sequences of precipitate coarsening in IN 718[1]. Recently, a number of programs including that of Collier et al have been initiated with the goal of being able to stabalize the precipitate phases of IN 718 against thermal instability and subsequent coarsening. Results of programs such as the above can be two fold: a) the life of a gas turbine engine component at existing temperatures may be extended to longer time periods or b) the component temperature may be increased resulting in increased gas turbine engine efficiency. Either of these will have a significant impact on civil transport costs.

Superalloys 718, 625 and Various Derivatives
Edited by Edward A. Loria
The Minerals, Metals & Materials Society, 1991

The goal of this program is two fold. The first and primary goal is to provide a fundamental analysis of the steady-state creep deformation mechanisms operating within a temperature regime where the γ'' phase is known to be unstable. This provides the baseline analysis by which a direct comparison of the results of the advanced alloy development programs can be made. The second goal of the program was to evaluate on a fundamental basis, the effect of age heat treatment on the steady-state creep deformation within the temperature regime corresponding to γ'' instability. Both heat treatments selected are well within the γ'' time-temperature regime with one heat treatment (depending on specific alloy composition) bordering on the γ' time-temperature regime.

Procedure

Material from an IN 718 ring forging was taken for the present study. The measured composition is given below.

Table I Chemical Composition of Alloy 718 in Weight Percent.

C	Mn	S	P	Si	Cr	Co	Mo	Ti
0.03	0.17	0.003	0.012	0.11	18.62	0.15	3.04	0.99
	Al	B	Ni	Cb+Ta	Mg	Ca	Fe	
	0.41	0.003	52.93	5.26	0.0005	0.0003	Rem	

Specimen blanks were given a one hour solution treatment at 1038°C followed by an oil quench to condition the material for aging. Two age heat treatments designated as heat treatment A and heat treatment B respectively were selected as follows:

Heat treatment A: 760°C 10hrs, F/C 38°C/hr to 650°C 10hrs, A/C
Heat treatment B: 718°C 8hrs, F/C 38°C/hr to 621°C 8hrs, A/C

Following the heat treatments, creep specimens consisting of threaded ends and a gage section measuring 6.35mm diameter by 30.48mm long were fabricated by low stress crush grinding. This specimen can be used for either creep testing or uniaxial tensile testing.

All creep tests were conducted on Satec Systems M3 constant load machines employing a lever arm ratio of 16:1. Test temperatures were achieved with Satec Systems three zone resistance heating furnaces attached to the creep machines. All creep machines are located in a temperature controlled room in order to minimize specimen temperature fluctuations throughout the day. All specimen temperatures were measured by placement of two Chromel Alumel type K thermocouples directly on the specimen gage section. All temperatures were controlled to within ±2°C of the desired test temperature. Creep tests were conducted in air at 650°C, 704°C and 760°C at constant initial applied stress levels ranging from 276 MPa up to 724 MPa. The creep strain was measured by means of dual dial gage averaging type extensometers attached to the shoulders of the creep specimens. All creep strain measurements reported are based on a 30.48mm gage length.

All tests were conducted well into the steady-state creep regime or regime corresponding to a minimum strain rate. When it was established that an accurate measurement of the steady-state strain rate could be obtained, the test was discontinued and the specimen was allowed to cool down to room temperature in the creep machine.

In addition to the creep testing, two specimens selected from each heat treatment were tensile tested. One at room temperature, and one at 650°C to verify response to heat treatment. The tensile tests were carried out in accordance with the procedures outlined in ASTM E 8 and ASTM E 21 for room temperature and elevated temperature tensile testing of metallic materials respectively.

Results

Heat Treatment and Microstructure

The solution treatment at 1038°C was employed for the purpose of taking all precipitated phases back into solution which were present from the prior forging plus heat treatment. Brooks and Bridges[3] have recently shown that any delta phase (orthorhombic Ni_3Nb), γ' or γ'' would re-solution at this temperature thus providing the optimum amount of Nb, Al and Ti for subsequent aging. In addition, the 1038°C solution treatment should result in a uniform constant grain size for all creep specimens, thus eliminating grain size as a variable influencing the creep behavior of the two age heat treatments. It was intended that the only variable influencing the creep behavior would be the precipitation heat treatment. The microstructure after the 1038°C solution treatment is shown in Figure 1. This heat treatment resulted in an average grain size of 150μm. It can be seen that no precipitate phases either at the grain boundaries or within the grain interrior are present such as the orthorhombic delta. The only phases present after the 1038°C solution treatment are dispersed carbides which would not disolve at this temperature. Thus, the microstructure shown in Figure 1 supports the data presented by Brooks and Bridges[3].

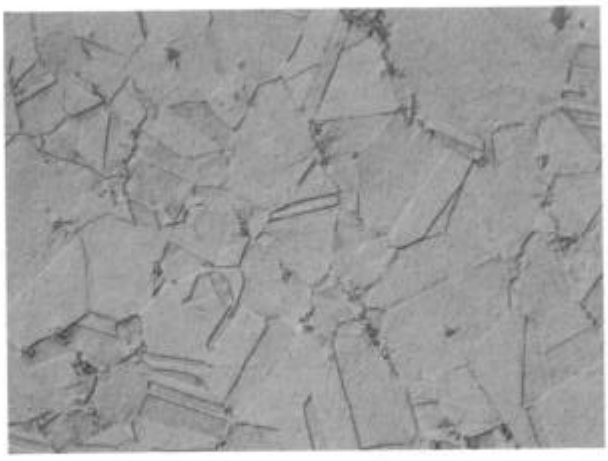

Figure 1: Optical microstructure of IN 718 following 1038°C solution treatment.

Tensile and Creep Behavior

As mentioned previously, a uniaxial tensile test was carried out at room temperature and at 650°C after each heat treatment to verify the material response to heat treatment prior to creep testing. The results are listed in Table II.

Table II Comparison of Tensile Properties of IN 718 as a Function of Age Heat Treatment

Heat Treatment	Temperature (°C)	0.2 Yld (MPa)	UTS (MPa)	EL (%)	RA (%)
A	Room	1171.9	1345.0	25	46
A	650°C	955.6	1112.7	23	34.9
B	Room	1072.7	1265.7	29	56.7
B	650°C	830.7	990.7	28	43.1

From the results of Table II, it appears that heat treatment A posseses properties which are superior to those of heat treatment B however, a firm establishment of this cannot be made with the limited data generated here. The properties of heat treatment A however, would conform to all of the commercial specification requirements for the tensile properties of IN 718 while the properties of heat treatment B would fall slightly below most commercial requirements. However, again it is emphasized that these observations are based on very limited data.

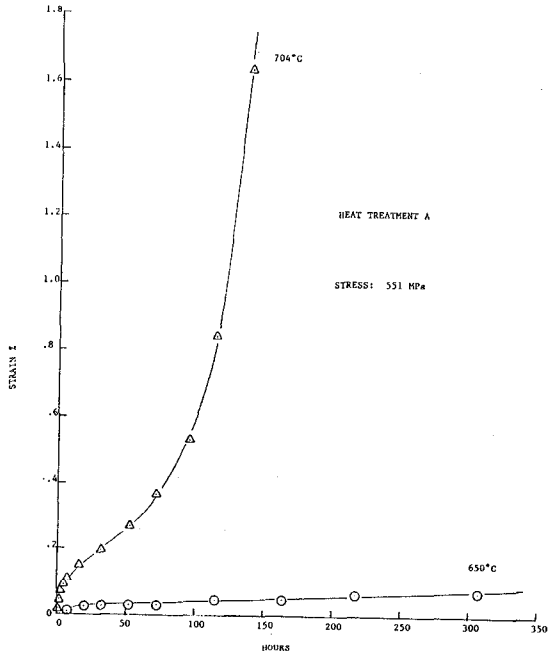

Figure 2: Creep Curves showing creep response of heat treatment A at 650°C and 704°C at an initial applied stress of 551 MPa.

The creep data is summarized in Table III. The results in Table III indicate that in most cases, the steady-state creep rate is lower at a given temperature and stress for heat treatment A than for heat treatment B. In all cases, the time to the onset of tertiary creep (t_t) is greater for heat treatment A. All creep curves exhibited a well pronounced primary creep regime. The extent of steady-state and tertiary creep (in those cases where tertiary was observed) varied depending on the temperature and stress level. A pair of typical creep curves for heat treatment A are shown in Figure 2. As indicated, the creep behavior is a strong function of the temperature at constant stress. The same behavior is expected by varying the stress at constant temperature.

Table III Summary of IN 718 Creep Data

H.T.	TEMPERATURE °C	STRESS MPa	STEADY-STATE CREEP Hr^{-1}	t_t Hr	t_r/DISC Hr
A	650	551	$1.3x10^{-6}$		308.5/DISC
B	650	551	$6.0x10^{-7}$		308.2/DISC
A	650	620	$3.0x10^{-6}$		283.9/DISC
B	650	620	$4.5x10^{-6}$	285	310.7/DISC
A	650	689	$1.39x10^{-5}$		95.0/DISC
B	650	689	$5.3x10^{-5}$	24	71.5/RUPT
A	650	724	$4.4x10^{-5}$	67	210.3/DISC
B	650	724	$1.0x10^{-4}$	6	24.9/DISC
A	704	483	$7.5x10^{-6}$		138.1/DISC
B	704	483	$9.0x10^{-6}$		137.9/DISC
A	704	517	$1.4x10^{-5}$		93.0/DISC
B	704	517	$3.26x10^{-5}$	64	93.0/DISC
A	704	551	$1.64x10^{-4}$	44	138.8/DISC
B	704	551	$1.23x10^{-4}$	19	50.1/DISC
A	704	620	$2.93x10^{-4}$	14	31.2/DISC
B	704	620	$4.15x10^{-4}$	3.2	14.8/RUPT
A	760	483	$8.0x10^{-4}$	3.0	15.5/RUPT
B	760	483	$1.76x10^{-3}$	1.8	11.9/RUPT
A	760	345	$1.42x10^{-5}$	58	88.8/DISC
B	760	345	$2.2x10^{-5}$	37	87.5/DISC
A	760	276	$1.8x10^{-6}$	88	147.1/DISC
B	760	276	$2.6x10^{-6}$	68	148.6/DISC
B	760	413	$1.92x10^{-4}$	9	40.8/RUPT

From the summary of data given in Table III, the stress and temperature dependence of the steady-state creep rate can be determined. A plot of log normalized stress (σ/E) vs log steady-state creep rate ($\dot{\epsilon}_{ss}$) for heat treatment A is presented in Figure 3. The temperature dependence of the un-relaxed dynamic Youngs modulus for IN 718 was obtained from ref 4. From Figure 3, it's shown that a linear stress dependence is obtained at all three test temperatures. In Figure 4, the log normalized stress vs log steady-state creep rate is plotted for heat treatment B. Again, a linear stress dependence is found at each test temperature with the slopes being nearly parallel as observed in Figure 3.

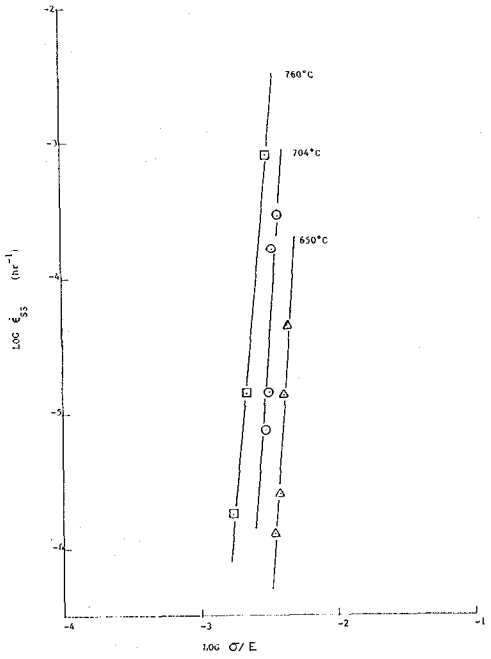

Figure 3: Stress dependence of the steady-state creep rate of IN 718 for heat treatment A.

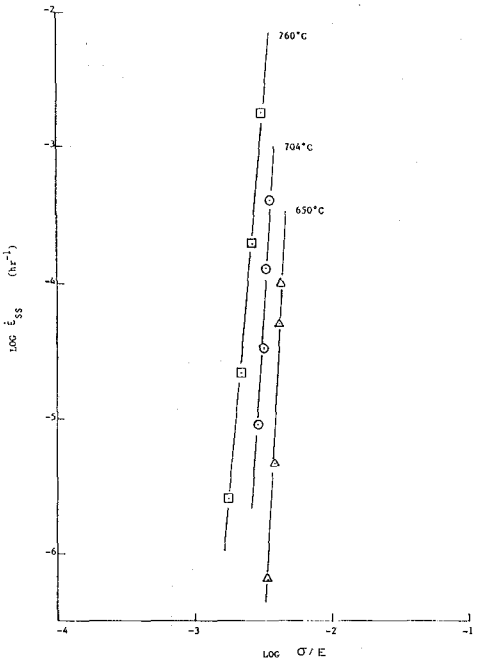

Figure 4: Stress dependence of the steady-state creep rate of IN 718 for heat treatment B.

Based on these results, the data in Figures 3 and 4 can be described well by the equation

$$\dot{\epsilon}_{ss} = K'\sigma^n \qquad (1)$$

where $\dot{\epsilon}_{ss}$ is the steady-state creep rate, K' is a material constant, σ is the applied creep stress and n is the apparent creep stress exponent. The values of n are given in Table IV.

Table IV Summary of Apparent Stress Exponents

HEAT TREATMENT	TEMPERATURE	STRESS EXPONENT
A	650°C	14.0
A	704°C	12.0
A	760°C	10.4
B	650°C	18.0
B	704°C	15.0
B	760°C	11.0

The stress dependence of the steady-state creep rates are high when compared to existing creep models. This observation is not uncommon with systems strengthened by second phase precipitates. Another significant observation is the tendency for the apparent stress exponent to decrease with increasing temperature as exhibited by both heat treatments. An Arrhenius plot of the log steady-state creep rate vs the reciprocal of the absolute temperature (1/T) at constant log normalized stress -2.45 for heat treatment A is shown in Figure 5. Calculation of the slope of this plot gives a modulus corrected creep activation energy of 554 kJ/mole. An Arrhenius plot of log steady-state creep rate vs 1/T at constant log normalized stress -2.45 is shown in Figure 6 for heat treatment B. The modulus corrected creep activation energy for heat treatment B was found to be 594 kJ/mole. For both heat treatments, the creep activation energy appears to be similar and independent of temperature within the temperature regime of this study. The creep activation energy in both cases is found to be significantly higher than the value for self diffusion in Ni which is on the order of 279 kJ/mole[5].

At 760°C, tertiary creep was observed at all stress levels employed for both heat treatments. In a previous study of the creep rupture behavior of the single crystal alloy Nasair 100, Nathal and Ebert[6] measured the stress dependence of the log time to the onset of tertiary creep (t_t). A plot of log time to the onset of tertiary creep vs log stress for heat treatments A and B at 760°C is presented in Figure 7. As shown in Figure 7, the slopes are parallel with the values being equal to 7.44. Following Nathal and Ebert, the present data can be described by the equation

$$t^t = A\sigma^n \qquad (2)$$

where t_t is the time to the onset of tertiary creep, A is a material constant, σ is the applied creep stress and ^{n} is the creep exponent. The value of 7.44 obtained for the IN 718 of this study is in reasonable agreement with the results reported by Nathal and Ebert for Nasair 100 at 925°C (6.0) and 1000°C (6.8)[6].

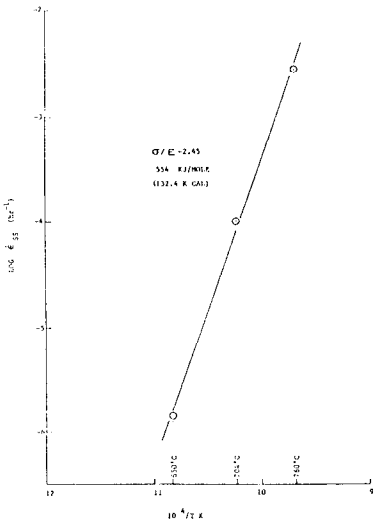

Figure 5: Arrhenius plot of the temperature dependence of the steady-state creep rate of IN 718 for heat treatment A.

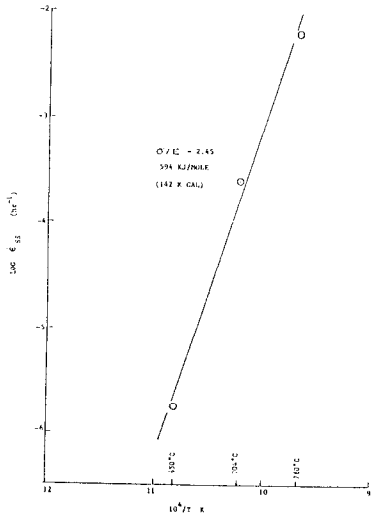

Figure 6: Arrhenius plot of the temperature dependence of the steady-state creep rate of IN 718 for heat treatment B.

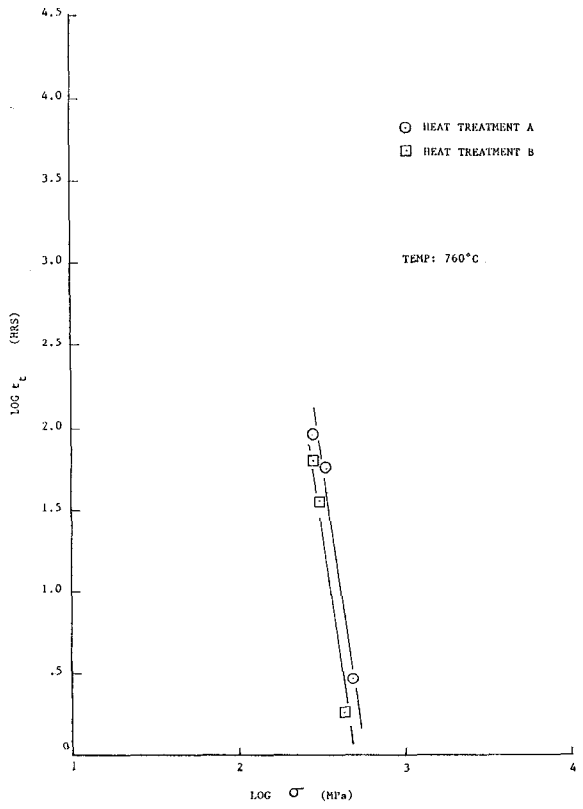

Figure 7: Stress dependence of the log time to the onset of tertiary creep of IN 718 for heat treatments A and B.

Discussion

Heat Treatment

The commercial heat treatments employed by industry to strengthen IN 718 result in an underaged condition[3]. The volume fraction of γ'' produced on aging at temperatures between 500°C and 700°C increases substantially with aging times up to 100 hours[3]. Conventional aging treatments such as heat treatment B of the present study generally result in a volume fraction of γ'' of about 13 percent as opposed to the theoretical maximum of 21 percent[3]. The sluggish aging response of IN 718 has been attributed to the slow diffusion of Nb which then implies a higher activation energy for diffusion of Nb in this alloy. From the results presented by Brooks and Bridges[3], it might be expected that the volume fraction of γ'' may be increased by aging at higher temperatures within the γ'' time-temperature regime while keeping the aging time comparable to that of the commercial heat treatment (heat treatment B). This was the basis for heat treatment A. The diffusivity of Nb is expected to increase within the higher temperature aging regime of heat treatment A thus possibly resulting in a higher γ'' volume fraction. In order to verify this, a quantitative measurement of the γ'' volume fraction would have to be made. From a qualitative standpoint, the higher tensile strength and in most cases, higher creep resistance exhibited by heat treatment A as compared to B suggest that a higher γ'' volume fraction may have resulted with heat treatment A.

Creep Deformation

Steady-State Creep

As shown in Figures 3-6, the high stress and temperature dependence of the steady-state creep rate persists for both heat treatments with the values of the creep stress exponents and activation energies appearing quite similar for each heat treatment. This suggests that the fundamental creep deformation process is controlled by the same mechanism for both heat treatments. When the values of the creep stress exponents and activation energies measured for the IN 718 are compared to those predicted by existing creep models, it is readily apparent that the present results cannot be described directly by the exitsting constitutive equations for creep[7]. As an example, the stress levels employed in the present study correspond to the dislocation climb controlled creep regime of 100μm grain size high purity Ni within the homologous temperature regime of the present study[8]. Thus, if climb is the assumed creep mechanism of the IN 718, then the power law creep equation

$$\dot{\epsilon}_{ss} = \frac{AD_L Gb}{kT} \left(\frac{\sigma}{E}\right)^5 \qquad (3)$$

where A is a structure dependent constant, D_L is the self diffusion coefficient, G is the shear modulus, b is the Burgers vector, k is Boltzman's constant, T is the absolute temperature and σ and E are as defined previously, would be appropriate for the creep data of the present study. Note that eqn. 3 predicts a creep activation energy (through the incorporation of D_L) equal to that of self diffussion (about 279 kJ/mole for Ni[5]) and a modulus compensated stress exponent of 5. Given the creep data of the present study, we must look to some mechanism other than climb at least as rate controlling for creep deformation of IN 718 within the temperature and stress regime of this study. We will first concentrate on the stress dependence of steady-state creep then proceed to the temperature dependence which will then be followed by a brief discussion of the tertiary creep behavior.

In a previous study of the influence of Nb additions to a Ni-Cr-Ti alloy strengthened by γ', Guo, Han and Yu[9] observed stress exponents comparable to those of the present study when creep testing at 700°C to 760°C at applied initial stress levels ranging from 392 MPa to 509.6 MPa. This temperature and stress regime envelopes that of the present study. Direct observation of the microstructures after creep testing by transmission electron microscopy (TEM) revealed that creep deformation proceeded by dislocations shearing the γ' particles along planar slip bands[9]. The element Nb when present in the γ', was shown to increase the long range order (LRO) parameter of γ' thus increasing the resistance of this phase to the passage of the dislocations[9]. Without the direct observation of deformation microstructures by means of TEM, it is not possible to specifically define the nature of the dislocation-particle interaction taking place during creep deformation of the IN 718. It is well established that the interaction between dislocations and a dispersed second phase can lead to stress exponents exceeding those predicted by existing constitutive equations for creep such as eqn. 3. In order to rationalize these high stress exponents, the concept of an effective stress for creep has been developed[10].

This concept has led to a modified power law equation of the form

$$\dot{\epsilon}_{ss} = A \left(\frac{\sigma - \sigma_R}{E}\right)^{n_0} \exp(-Q/RT) \qquad (4)$$

where σ_R is a threshold stress for creep deformation and n_0 is the value of the stress exponent in the absence of the second phase giving rise to the threshold stress. Thus if an accurate measurement of the threshold stress can be obtained, eqn. 4 can be used to describe the basic creep deformation process and for climb controlled creep, would result in a creep stress exponent and activation energy as predicted by eqn. 3. The concept of an effective stress for creep has been employed with success to rationalize the high creep stress exponents and activation energies measured for the oxide dispersion strengthened (ODS) superalloys[11]. Although the threshold stress was not estimated in the present study, we believe that the high stress exponents measured can be rationalized in terms of the presence of the γ'' precipitates and reflect the resistance against creep deformation excerted by these precipitates.

A very significant observation with respect to the dislocation-precipitate particle interaction during creep of the IN 718 is the tendency of the stress exponent to decrease as the creep temperature increases from 650°C to 760°C. Within this temperature regime the γ'' is known to be unstable and thus is expected to coarsen and begin to revert to the more stable orthorhombic delta phase[1-3]. Superimposition of the applied creep stress should accelerate coarsening kinetics. We believe that the decreasing stress exponent with increasing temperature reflects the coarsening of the γ''. As coarsening progresses, the ability of the precipitates to impede dislocation motion during creep deformation decreases and the stress exponent decreases back down to the value expected for creep in the absence of the precipitate particles (eqn. 3). The microstructure of a creep specimen of heat treatment A tested at 760°C and 345 MPa is shown in Figure 8. In this micrograph, planar slip bands can be seen indicating that dislocation motion was indeed present during creep deformation.

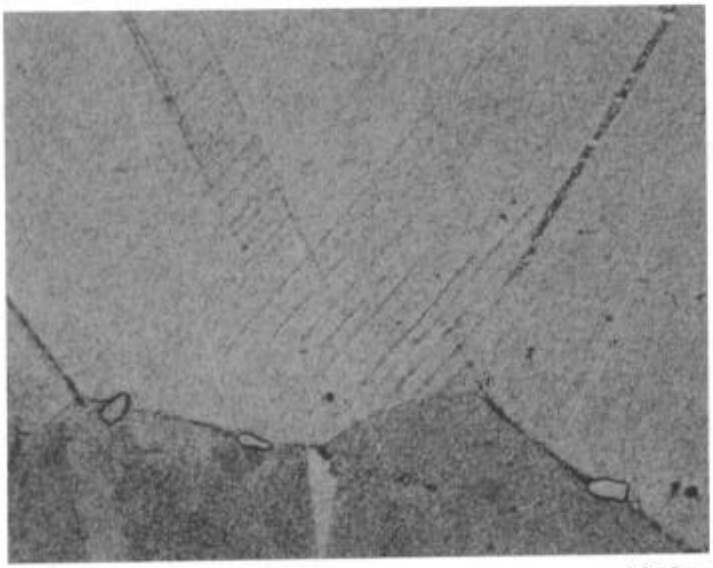

Figure 8: Optical microstructure of IN 718 (heat treatment A) from the gage section of a creep specimen tested at 760°C and 345 MPa. Creep test was conducted well into the tertiary creep regime.

Another possibility for the decreasing stress dependence of steady-state creep with increasing temperature is the onset of a diffusional creep process with increasing temperature. If diffusional creep either by the Nabarro-Herring or Coble process were to contribute to creep deformation taking place by dislocation climb, the power law stress exponent would decrease resulting in a stress exponent reflecting the contribution of both diffusional and dislocation creep to the overall deformation process. The constitutive equations for both Nabarro-Herring and Coble creep each predict a stress exponent of 1.

Focusing now on the temperature dependence of steady-state creep, we note that the creep activation energies exceed the value of self diffusion in Ni by a substantial margin. We see again that the present creep activation energies do not conform well to the existing constitutive models of creep which in most cases predict a value equal to that of self diffusion in the base material[7]. It is well established that the presence of microstructural instabilities during creep deformation can have a significant impact on the measured creep activation energy. If creep testing is performed under these conditions, the microstructural instabilities must be accounted for in the analysis of the data. As discussed in the previous section, such is the case of the present study. In a previous study, Guo, Han and Yu[9] measured the creep activation energy of a Ni-Cr-Ti alloy as a function of Nb additions and found a linear increase in activation energy with increasing Nb. This data is re-plotted in Figure 9 along with the creep activation energies obtained in the present study. As indicated in Figure 9, the present results for IN 718 having 5.26 weight percent Nb fall on the data of Guo, Han and Yu when extrapolated out to the weight percent Nb of IN 718. This is an indication that the high creep activation energies measured for the IN 718 may be rationalized on the basis of the high Nb content of this alloy. Under the present creep conditions, it is most likely that the creep deformation rate is controlled by the rate of γ'' coarsening rather than the creep deformation process itself.

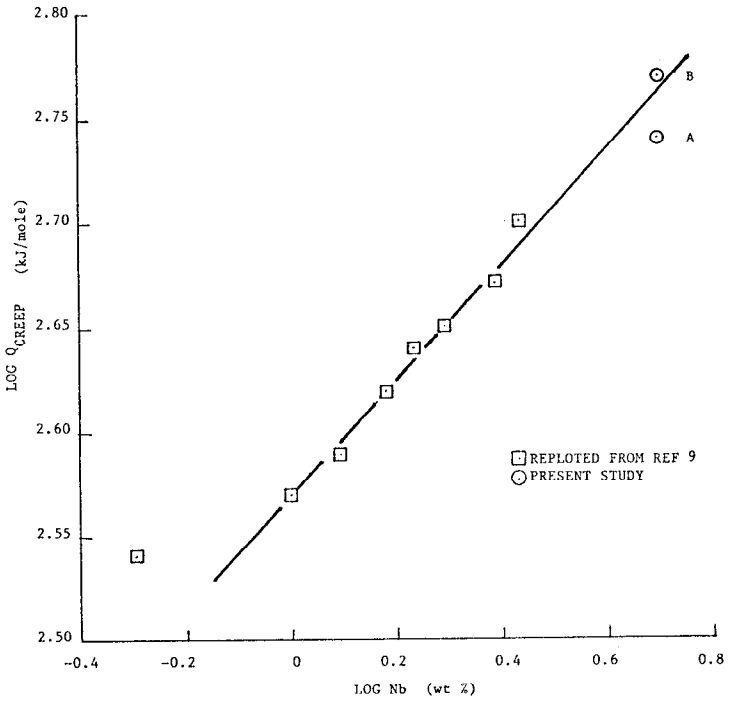

Figure 9: Plot of log Nb concentration versus the log of the creep activation energy. Data replotted from Guo, Han and Yu (ref 9) along with IN 718 creep activation energies from present study.

The high activation energies measured are thus postulated to reflect the diffusion of Nb through the gamma matrix as γ'' coarsening progresses. The above arguement is based on the fact that the γ'' coarsening rate will directly effect the creep deformation rate thus giving rise to an in series process whereby the slowest rate process having the highest activation energy will control[12].

Tertiary Creep

In a recent study, Dyson and Gibbons present an analysis of experimental data and a theoretical synthesis of tertiary creep in Ni-based superalloys[13]. It is established that the extended period of tertiary creep in Ni-based superalloys having high ductility (El>10 pct.) is not due to the thermal instability of the particulate microstructure but rather is due to a strain induced instability of the dislocation substructure developed during creep deformation[13]. This is a feature which appears to be intrinsic to the Ni-based superalloys. This substructure instability results in an accumulation of strain which leads to the upward rise of the strain vs time curve known as tertiary creep. Although the precise micro-mechanisms are not well established at present, it has recently been suggested that for superalloys strengthened by γ', the acceleration in strain accumulation may be influenced by the volume fraction of the γ' particles and the magnitude of their lattice parameter mismatch with the matrix[13]. In contrast to the above, in low ductility superalloys (El<2 pct.) grain boundary cavitation appears to be the dominant process giving rise to the onset of tertiary creep. Preliminary metallographic results of the present study indicates that tertiary creep under the present creep conditions may be dominated by the intrinsic strain accumulation due to dislocation substructure instability. In support of this is the fact that IN 718 within the temperature range of 650°C to 760°C has excellent ductility. Also note that in Figure 8, no evidence of grain boundary cavitation can be found in a specimen crept well into the tertiary creep regime. In aggreement with the suggested variables giving rise to substructure instability, the volume fraction decrease of the γ'' resulting from coarsening within the creep temperature regime may be expected to lead to an acceleration of strain accumulation[13].

In Figure 7, the stress dependence of the time to the onset of tertiary creep of each heat treatment is shown. The results depicted in Figure 7 of the present study follow exactly the same trend shown by Nathal and Ebert for single crystal Nasair 100[6]. In their study, it was shown that directional coarsening of the γ' into a rafted morphology played a major role in inhibiting dislocation motion in Nasair 100 during creep deformation at 1000°C[6]. The activation energy for creep was found to be comparable to the measured activation energy for Ostwald Ripening in this alloy. The stress dependence of the time to the onset of tertiary creep can be thought of as a stress dependence of the time to the onset of some instability giving rise to an enhancement in creep dislocation mobility. In the case of the present IN 718, this would reflect γ'' coarsening to the extent that an easy mean free path develops allowing the necessary strain accumulation to take place. It should be emphasized that a more detailed systematic study of the tertiary creep process of IN 718 is needed in order to correlate the behavior of this alloy with the behavior cited for γ' strengthened superalloys in ref 13.

Conclusions

Following a 1038°C solution treatment, an aging heat treatment consisting of 760°C/10 hours F/C to 650°C/10 hours resulted in superior tensile properties at room temperature and at 650°C as well as superior creep resistance within the temperature regime of 650°C to 760°C when compared to material aged at 718°C/8 hours F/C to 621°C/8 hours which is the commercial aging treatment for IN 718. The improvement in creep resistance consisted of lower steady-state creep rates and longer times to the onset of tertiary creep. It is suggested that a higher γ'' volume fraction may have resulted from aging at higher temperature cycles within the γ'' time-temperature regime over comparable time periods to those of the commercial age treatment.

The stress and temperature dependence of the steady-state creep rate of IN 718 was found to exceed typical values predicted by existing constitutive creep equations for power law creep and could therefore not be discribed by such equations. The high stress exponents measured for both heat treatments are suggested to reflect the resistance to dislocation motion during creep deformation imparted by the γ'' precipitate particles. Within the creep temperature regime of 650°C to 760°C, γ'' precipitate particle coarsening takes place giving rise to a decrease in the stress exponent with increasing temperature observed for both age heat treatments. The high creep activation energies measured are suggested to represent the rate controlling creep mechanism which in the present case is postulated as being the coarsening rate of the γ'' particles.

Finally, tertiary creep under the present creep conditions for γ'' strengthened IN 718 may take place by a mechanism of strain induced dislocation substructure instability which has been demonstrated for a number of γ' strengthened Ni-based superalloys. The dislocation substructure instability may relate to the change in γ'' volume fraction which occurs as a result of the coarsening of this phase within the creep temperature regime.

Acknowledgements

The author would like to express appreciation to Carlton Forge Works for providing the Inconel alloy 718 material for this program.

References

1. J.P. Collier, A.O. Selius and J.K. Tien, Superalloys 1988 (Conference Proceedings) TMS-AIME, 1988 p 43.

2. D.F. Paulonis, J.M. Oblak and D.S. Duvall, Trans ASM, 62, 1969, p 611.

3. J.W. Brooks and P.J. Bridges, Superalloys 1988 (Conference Proceedings) TMS-AIME, 1988, p 33.

4. Rockwell International Corp, Rocketdyne Division, Materials Properties Handbook, Vol II, 1977.

5. J.E. Dorn, Creep and Recovery (Conference Proceedings) ASM, 1957, p 255.

6. M.V. Nathal and L.J. Ebert, Met Trans A, 16A, 1985, p 427.

7. A.K. Mukherjee, J.E. Bird and J.E. Dorn, Trans ASM, 62, 1969, p 155.

8. M.F. Ashby, The Microstructure and Design of Alloys, Proceedings, Third International Conference on Strength of Metals and Alloys, 2, Cambridge, England, 1973, p 8.

9. E. Guo, Z. Han and S. Yu, Superalloys, 1984 (Conference Proceedings) TMS-AIME, 1984, p 583.

10. S. Purushothaman and J.K. Tien, Acta Metall, 26, 1978, p 519.

11. V.C. Nardone, D.E. Matejczyk and J.K. Tien, Acta Metall, 32, 1984, p 1509.

12. G. Schoeck, Creep and Recovery (Conference Proceedings), ASM, 1957, p 199.

13. B.F.Dyson and T.B. Gibbons, Acta Metall, 35, 1987, p 2355.